Circulation

Real-Time Catheter Molecular Sensing of Inflammation in Proteolytically Active Atherosclerosis

Farouc A. Jaffer, Claudio Vinegoni, Michael C. John, Elena Aikawa, Herman K. Gold, Aloke V. Finn, Vasilis Ntziachristos, Peter Libby and Ralph Weissleder

The online version of this article, along with updated information and services, is located on the World Wide Web at:

http://circ.ahajournals.org

Data Supplement (unedited) at:

http://circ.ahajournals.org/cgi/content/full/CIRCULATIONAHA.108.785881/DC1

Imaging

Real-Time Catheter Molecular Sensing of Inflammation in Proteolytically Active Atherosclerosis

Farouc A. Jaffer, MD, PhD; Claudio Vinegoni, PhD; Michael C. John, MPH; Elena Aikawa, MD, PhD;
Herman K. Gold, MD†; Aloke V. Finn, MD; Vasilis Ntziachristos, PhD;
Peter Libby, MD; Ralph Weissleder, MD, PhD

Background—To enable intravascular detection of inflammation in atherosclerosis, we developed a near-infrared fluorescence (NIRF) catheter–based strategy to sense cysteine protease activity during vascular catheterization.

Methods and Results—The NIRF catheter design was based on a clinical coronary artery guidewire. In phantom studies of NIRF plaques, blood produced only a mild ($<30\%$) attenuation of the fluorescence signal compared with saline, affirming the favorable optical properties of the NIR window. Catheter evaluation in vivo used atherosclerotic rabbits ($n=11$). Rabbits received an injection of a cysteine protease–activatable NIRF imaging agent (Prosense750; excitation/emission, 750/770 nm) or saline. Catheter pullbacks through the blood-filled iliac artery detected NIRF signals 24 hours after injection of the probe. In the protease agent group, the in vivo peak plaque target-to-background ratio was 558% greater than controls (6.8 ± 1.9 versus 1.3 ± 0.3, mean$\pm$SEM; $P<0.05$). Ex vivo fluorescence reflectance imaging corroborated these results (target-to-background ratio, 10.3 ± 1.8 for agent versus 1.8 ± 0.3 for saline group; $P<0.01$). In the protease group only, saline flush–modulated NIRF signal profiles further distinguished atheromata from normal segments in vivo ($P<0.01$). Good correlation between the in vivo and ex vivo plaque target-to-background ratio was present ($r=0.82$, $P<0.01$). Histopathological analyses demonstrated strong NIRF signal in plaques only from the protease agent group. NIRF signals colocalized with immunoreactive macrophages and the cysteine protease cathepsin B.

Conclusions—An intravascular fluorescence catheter can detect cysteine protease activity in vessels the size of human coronary arteries in real time with an activatable NIRF agent. This strategy could aid in the detection of inflammation and high-risk plaques in small arteries. (***Circulation***. 2008;118:000-000.)

Key Words: atherosclerosis ■ catheters ■ fluorescence ■ imaging ■ inflammation ■ cathepsins

Extensive preclinical and clinical investigations of atherosclerosis link inflammation to plaque progression and complications.[1] Although several imaging methods can assess plaque structure, few can visualize specific molecular and cellular aspects of the inflammatory process. To address this need, rapidly developing molecular sensing strategies may permit visualization of key biological processes in atherosclerosis.[2,3]

Clinical Perspective p ●●●

In particular, near-infrared fluorescence (NIRF) detection strategies can visualize inflammatory processes in atheromata of small animals, including cysteine proteinase and matrix metalloproteinase activity.[4,5] Given the role of altered protease activity in atheroma expansion and destabilization,[6–8] visualization of atheroma protease activity in human subjects might identify inflamed, high-risk lesions associated with myocardial infarction.[9]

To date, no readily translatable platform for the detection of NIRF signal from atheromata in vivo exists. To address this need, we have developed a flexible, narrow-diameter NIRF catheter to permit in vivo, intravascular NIRF sensing in human coronary artery–sized vessels. Here, we investigated the ability of the NIRF catheter to visualize protease activity indicative of inflammation in real time in vivo in rabbit atheromata, the effects of blood absorption on the in vivo NIRF signal, and the association between in vivo NIRF signals and histological measures of inflammation, specifically plaque cysteine proteases and macrophages.

Methods

NIRF Catheter

The custom-built catheter-based sensing system is compact and consists of few components. A continuous-wave laser diode with an
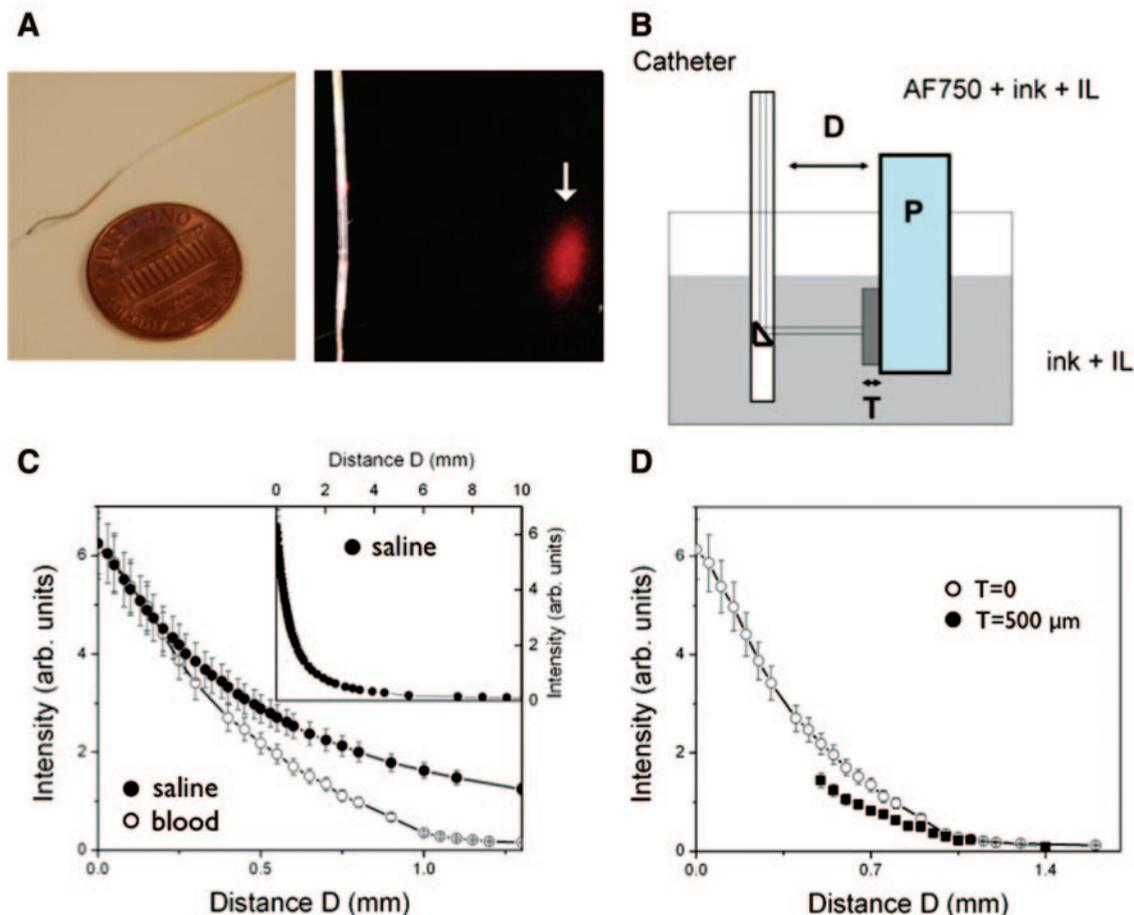
Figure 1. The NIRF catheter prototype. A, The catheter consists of a 0.36-mm/0.014-in floppy radiopaque tip with a maximum OD of 0.48 mm/0.019 in. The focal spot for the 90° arc-sensing catheter was 40 ± 15 μm at a working distance of 2 ± 1 mm (arrow). B, Phantom for intravascular simulation measurements. Plaque (P) consists of intralipid plus India ink 50 plus AF750 (NIR fluorochrome); tissue (T; fibrous cap) consists of polyester casting resin plus titanium dioxide (TiO_2) plus India ink; the container (gray shaded area) was filled with fresh rabbit blood or saline. The catheter was immersed in fresh rabbit blood and positioned at a variable distance (D) from a fluorescent phantom representing the plaque (P). To mimic the presence of a fibrous cap, a solid tissue phantom of thickness T was interposed between the plaque and the lumen. C, Plot of the detected NIRF signal as a function of the distance D in the presence of blood (1/e signal decay, 500 μm; $\circ$) compared with saline (1/e signal decay, 700 μm; $\bullet$). Inset, The fluorescence signal decay in saline at distances up to 10 mm. D, Plot of the detected NIRF signal in blood in the presence of a tissue phantom (T) of thickness 500 μm shows modest NIRF signal attenuation (<35%) vs the case in C where T=0.

excitation wavelength of 750 nm (B&W TEK, Newark, Del) served as an excitation source. The excitation light was filtered with a narrow-bandpass interference filter centered at 752 nm and with a 5-nm full width at half-maximum to remove any residual laser scatter. Next, filtered excitation light was guided with a multimode fiber after passing through a 3-dB beam splitter and then coupled into a dedicated catheter prototype based on an optical coherence tomography wire (LightLab Imaging Inc, Westford, Mass). The catheter contains a 0.36-mm/0.014-in floppy radiopaque tip with a 0.41-mm/0.016-in OD housing a 62.5/125-μm multimode fiber 200 cm long. The smaller diameter and greater flexibility represented a significant advance over our prior proof-of-principle NIRF catheter design with application limited to large-caliber ex vivo structures.[10] At the end of the catheter, a prism then directed the light at 90° with respect to the catheter and focused this light on a near diffraction-limited focal spot size of $\approx40\pm15$ μm at a working distance of 2 ± 1 mm (Figure 1A). Emitted fluorescent light was then collected back into the catheter and guided to the beam splitter, where one half of the photon flux was coupled into a separate multimode fiber. To limit contamination by backscattered light, fluorescence photons were filtered with a dielectrically coated dichroic filter with a cut-on wavelength of 780 nm. The residual fluorescence light was detected with a photomultiplier tube (H5783-20, Hamamatsu, Shizuoka,

Japan) and then digitized with 16-bit resolution at 1 kHz (DAQ card, National Instruments, Austin, Tex) operating on a personal computer. Data noise reduction was performed with a 50-point moving average filter (MatLab version 7.5, MathWorks, Natick, Mass). The present studies typically used laser powers of 0.9 mW as measured by a power meter at the catheter tip, considerably lower than the 5- to 15-mW power used in clinical optical coherence tomography systems.[11]

Phantom Experiments

An atherosclerotic vessel phantom was designed that consisted of fresh whole rabbit blood, simulated tissue, and plaque (Figure 1B). The plaque was simulated with a cuvette filled with a solution of 1% intralipid (Liposyn, Hospira Inc, Lake Forest, Ill) and 50 ppm India ink.[12] The plaque was rendered fluorescent with an NIR fluorochrome (AF750, Molecular Probes, Inc, Eugene, Ore) at a concentration of 300 nmol/L. The overlying solid tissue phantom was made from a polyester casting resin (Castin'Craft, ETI, Fields Landing, Calif) mixed with TiO_2 (Sigma-Aldrich Chemical Co Inc, Milwaukee, Wis) and India ink (Faber-Castell, Cleveland, Ohio)[12] to mimic typical tissue optical properties in the NIR.[13] The optical parameters of the tissue were chosen to produce lower absorption and increased scattering compared with blood ($\mu_a=0.4$ cm^{-1} and $\mu'_s=12$ cm^{-1},

respectively). The tissue thickness was varied to be 0 (no tissue phantom present) or 500 μm.

The catheter was next immersed in the vessel phantom at a distance from the fluorescent plaque. The optical power at the exit of the catheter was kept fixed during all the measurements at 0.9 mW. The fluorescence intensity was recorded with the system described above.

Cysteine Protease–Activatable Imaging Agent

A cysteine protease–activatable NIRF agent with utility in atherosclerosis was used[4,14] and scaled up for large-animal use (Prosense750; excitation/emission, 750 nm/780 nm; VisEn Medical, Woburn, Mass). The agent consists of multiple NIR fluorochromes linked to protected graft copolymer consisting of lysine-lysine bonds. At baseline, the agent is minimally fluorescent because of intramolecular quenching. The agent reports on cysteine proteases, including cathepsin B.[4,14,15] After cleavage by cysteine proteases, the backbone liberates smaller fragments with dequenched NIR fluorochromes, generating strong local fluorescence. For further details on this class of activatable imaging agents and the mechanism of NIRF signal generation, see the discussion by Jaffer et al.[16]

Atherosclerosis

New Zealand white rabbits (weight, 3 to 3.5 kg; Charles River Laboratories, Wilmington, Mass) underwent balloon denudation of iliac arteries and hypercholesterolemic diet to produce inflamed atheromata. Rabbits consumed a high-cholesterol diet (1% cholesterol and 5% peanut oil, C-30293, Research Diets, Inc, New Brunswick, NJ) for 1 week before balloon injury. After an overnight fast, anesthesia was induced with intramuscular ketamine (35 mg/kg) and xylazine (5 mg/kg). Anesthesia was continued with inhaled isoflurane (1% to 5% vol/vol, Baxter, Deerfield, Ill) and supplemental O_2. Next, a 3F Fogarty arterial embolectomy catheter (Edwards Lifesciences, Irvine, Calif) was advanced into the common iliac vessels. The balloon was inflated to tension (0.6 to 1.0 mL). A total of 3 pullbacks were performed in the left and right iliac arteries and in the infrarenal aorta. After injury, the introducer was removed, and the left carotid artery was ligated. Rabbits continued on the high-cholesterol diet for 4 to 8 weeks. Plasma cholesterol levels were measured with a commercial kit (Hemagen, Columbia, Md). Twenty-four hours before in vivo experiments, rabbits received the protease agent (600 nmol/kg) or saline intravenously. This postinjection time point was chosen on the basis of prior experimental results with protease-activatable agents in atherosclerosis.[4,16]

Intravascular Sensing of NIRF Signals in Atherosclerosis

Anesthesia was initiated as above, and a 5F introducer was placed in the right carotid artery and then delivered to the descending thoracic aorta under fluoroscopic guidance. Intravenous heparin (150 U/kg) was administered next. A 5F balloon wedge catheter (Arrow International Inc, Reading, Pa) was placed through the sheath and advanced to the abdominal aorta, followed by aortoiliac angiography. The NIRF catheter was then advanced through the balloon wedge catheter into the distal iliac arteries. To limit sampling variability from the 90° sensing catheter, manual pullback of the catheter over 20 seconds was performed in each iliac artery 3 times. From each digitized pullback, the maximum voltage was recorded. From this set of maximum voltages, the maximal value was identified. The in vivo plaque target-to-background ratio (TBR) was thus calculated as maximum voltage detected from all pullbacks divided by background voltage.

To confirm that the augmented voltage was plaque specific, the catheter was readvanced to lesions with the angiogram and NIRF signal used as a roadmap. The static voltage was recorded adjacent to plaques and adjacent to the normal-appearing vessel wall on angiography. To assess the effect of blood absorption on the detected NIRF signal, balloon occlusion and saline flushing (3 mL over 4 seconds) were performed through the balloon wedge catheter (Arrow International Inc). Flushing and associated voltage traces were recorded in both areas of plaque and normal vessels. After completion of the experiment, rabbits were killed, and blood was obtained and anticoagulated (9 parts blood, 1 part 3.8% sodium citrate). The rabbit was then perfused with saline and 4% paraformaldehyde at physiological pressure. The institutional Subcommittee on Research Animal Care approved all animal protocols.

Ex Vivo Imaging

Resected atherosclerotic aortoiliac vessels underwent fluorescence reflectance imaging (FRI) with an excitation/emission filter of 762 nm/800 nm and a 5-second exposure time (BonSAI, Siemens, Erlangen, Germany). Light images also were obtained with an exposure time of 100 ms. Region-of-interest analysis was performed with visual identification of plaques and normal background on FRI images (Osirix version 2.7.5, A. Rosset). The plaque TBR was defined as plaque region-of-interest signal divided by adjacent vessel background region-of-interest signal).

Histopathology

After imaging, vessels were immersed in 4% paraformaldehyde for 24 hours. Vascular rings were then frozen in optical cutting temperature compound (Sakura Finetek, Torrance, Calif) for histopathological analysis. Serial 5-μm cryosections of rabbit atheromata were cut. Immunohistochemistry was performed using the avidin-biotin-peroxidase method. Briefly, sections treated with 0.3% hydrogen peroxide were incubated for 60 minutes with primary or isotype control antibodies, followed by the respective biotinylated secondary antibody. The reaction was visualized with aminoethylcarbazole substrate (Dako, Carpinteria, Calif) and counterstained with Harris hematoxylin solution. Immunoreactive cathepsin B was detected with a polyclonal goat anti–cathepsin B antibody (Santa Cruz Biotechnology, Santa Cruz, Calif). Plaque macrophages were identified with a mouse monoclonal antibody (Ab-5/RAM-11, Laboratory Vision, Fremont, Calif). Tissue sections were viewed with a microscope (Nikon Eclipse 50i, Tokyo, Japan), and images were captured with a CCD-SPOT RT digital camera (Diagnostic Instruments, Sterling Heights, Mich).

Fluorescence Microscopy

Cryosections (5 μm) were obtained from fresh-frozen rabbit arteries. Fluorescence microscopy of plaque and normal vessel sections was performed with an upright epifluorescence microscope (Eclipse 80i, Nikon) that visualized the distribution of agent-specific NIRF (excitation, 673 to 748 nm; dichroic mirror, DM750; emission, 765 to 835 nm; exposure time, 5 seconds) and autofluorescence (excitation, 460 to 500 nm; dichroic mirror, DM505; emission, 510 to 560 nm; exposure time, 0.5 second).

Statistical Analysis

Data are presented as mean±SE. Student t test was used to compare the mean TBR between the protease agent group and saline group for both in vivo and ex vivo fluorescence studies. Linear regression was performed with Prism version 4.0c (GraphPad Software, San Diego, Calif). A value of $P<0.05$ was considered statistically significant.

The authors had full access to and take full responsibility for the integrity of the data. All authors have read and agree to the manuscript as written.

Results

Light Attenuation in Blood and Tissue Phantoms In Vitro

Light attenuates considerably while traveling through opaque tissue, but the NIR window used here minimizes photon attenuation. Modeling of the effects of blood and tissue on NIRF signal attenuation used an atherosclerotic vessel wall phantom that consisted of fresh blood, simulated tissue, and NIRF plaque (Figure 1B). In vitro modulation of the distance,
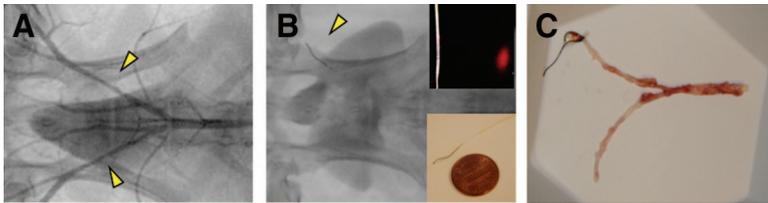
Figure 2. In vivo catheter placement in experimental atherosclerosis of New Zealand white rabbits. A, Angiography of balloon-injured, cholesterol-fed rabbits revealed visible lesions in the iliac arteries (arrowheads). B, The NIRF catheter guidewire was easily delivered past stenoses in the iliac arteries (arrowhead). C, Gross pathology revealed yellow-white atheromata in injured areas in the iliac arteries.

reflecting the blood volume between the catheter and the plaque, produced mild NIRF signal attenuation in the presence of blood, with a decay distance (1/e) of 500 μm compared with a decay distance of 700 μm in saline (Figure 1C). Modeling in the visible light range indicated significantly greater photon attenuation (data not shown). The tissue thickness, reflecting a simulated fibrous cap overlying the fluorescent plaque, showed instead only modest effects on the NIRF signal with a 500-μm thickness (Figure 1D). These blood and tissue attenuation curves demonstrated feasibility of light detection through blood in the NIR window.

Delivery of the Intravascular NIRF Catheter in Atherosclerotic Vessels

Balloon injury of the iliac arteries, followed by hypercholesterolemia (average cholesterol, 1077±672 mg/dL), induced angiographically visible lesions with evident luminal narrowing (angiographic stenosis, 30% to 100% diameter; Figure 2A). Total occlusions (100% stenosis) were noted in 3 of 22 (14%) of the injured iliac arteries. In patent arteries, the NIRF catheter was easily advanced bare wire through a 5F balloon wedge pressure catheter and selectively placed in the right or left iliac artery as desired (Figure 2B). Resected aortoiliac vessels after the imaging procedure showed bilateral yellowish-white atheromata in areas of balloon injury (Figure 2C).

Real-Time Intravascular Detection of NIRF Signals Through Flowing Blood

All animals tolerated injection of the protease-activatable agent; no adverse events were noted. To measure the plaque-

associated NIRF signal in vivo, distal-to-proximal pullbacks of the iliac vessels and abdominal aorta were performed in each iliac artery (Figure 3 and Movie I of the online-only Data Supplement). Pullbacks were performed during flowing blood without occlusion or flushing. The maximal voltage was recorded from 3 distinct catheter pullbacks to maximize the sampled vessel area. Study of animals that received the cysteine protease–activatable agent yielded high levels of NIRF (voltage) (Figure 3). The augmented NIRF signal localized to plaques as assessed by x-ray angiographic correlation and by direct repositioning of the NIRF catheter at plaques defined by angiography. The peak in vivo plaque TBR was 6.8±1.9 in the protease agent group. In contrast, control animals showed minimal change in the baseline low NIRF signal during pullbacks (Figure 3). The peak in vivo plaque TBR was 1.3±0.3 ($P<0.05$), consistent with low plaque autofluorescence in the NIR window.[17] Overall, the protease-activatable agent produced a 558% higher plaque TBR than plaques from the saline group.

Distinctive NIRF Signal Profiles Further Distinguish Plaques From Normal-Appearing Vessels

To assess the specificity of plaque NIRF signal in the protease agent group, the catheter was readvanced to atheromata or normal-appearing segments as defined by the angiogram. Stationary recordings demonstrated augmented NIRF signal in the region adjacent to plaques compared with normal areas and showed that the NIRF signal was stable during physiological pulsatile blood flow (Figure 4). Modest quenching (<30% reduction in the fluorescence signal at 5
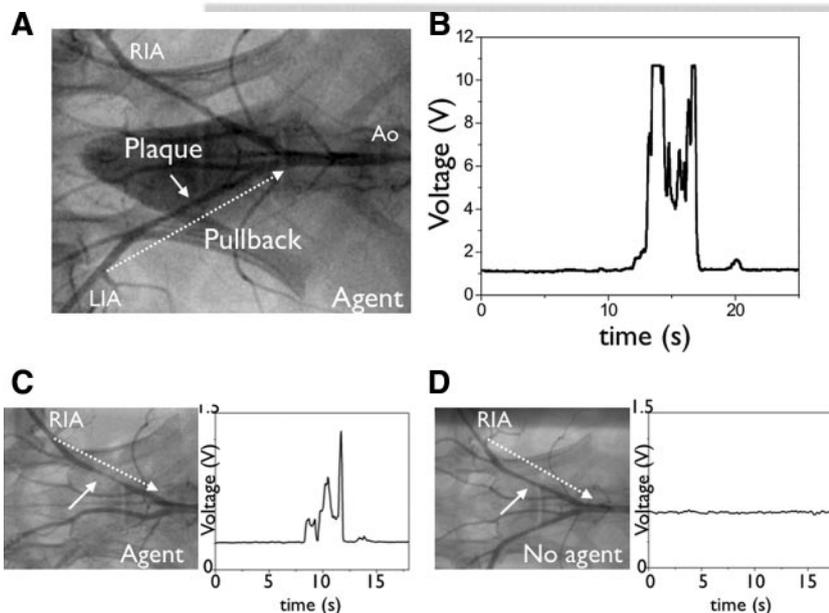

Figure 3. Real-time, in vivo fluorescence sensing of inflammation in atherosclerotic vessels. A, Repeated manual pullback of the catheter was performed in each iliac distally to proximally over 20 seconds (dotted arrow; see also the Movie in the online-only Data Supplement). B and C, In rabbits that received the NIRF protease-activatable agent 24 hours beforehand (active group), strong NIRF signal (average TBR, 6.8) was detected as the catheter pulled back across the plaque defined by the angiogram. Catheters were readvanced to lesions, and stationary recordings confirmed augmented NIRF signal. D, In control saline-injected rabbits, minimal NIRF signal deviation was detected during catheter pullback. RIA indicates right iliac artery; LIA, left iliac artery; and Ao, aorta.
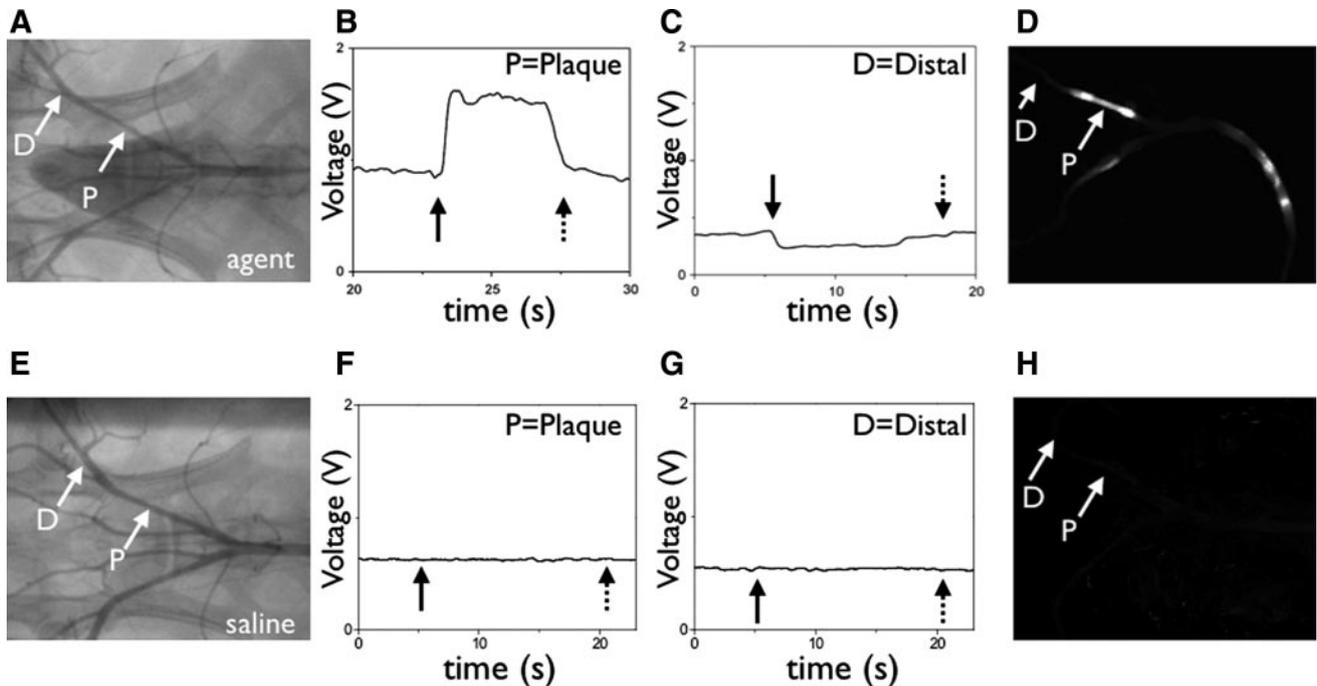
Figure 4. Effect of blood absorption on catheter-detected NIRF signals. In vivo NIRF signal profiles of protease agent and control rabbits under conditions of blood displacement (via balloon occlusion and saline flushing). The NIRF catheter was positioned adjacent to a plaque or distal reference segment. A, Angiogram of a rabbit receiving the protease agent ("active") revealing bilateral iliac artery plaques. B, With the catheter positioned at the right iliac artery plaque, blood displacement via saline flushing augmented the peak NIRF signal (average, 74%), as predicted by the phantom studies. C, In contrast, in normal vessel areas, saline flushing reduced the NIRF signal by 38% ($P<0.01$), consistent with the displacement of the low-level background fluorescence produced by the circulating, unactivated imaging agent. D, Corresponding ex vivo fluorescence reflectance image demonstrating strong NIRF signal in the plaque but not distal reference segment. E, Angiogram of a control animal showing bilateral iliac artery plaques. F and G, In control animals, blood displacement did not alter the NIRF signal in areas of plaques or normal segments. H, Negligible NIRF signal was evident on corresponding ex vivo FRI. Images in D and H windowed identically. In addition, the NIRF signal remained stable during acquisition through physiological blood flow in both Prosense-injected and control animals and in both areas of plaques and distal reference segments (dotted line region before balloon inflation in B, C, F, and G). For B, C, F, and G, closed arrow indicates the start of balloon occlusion and saline flushing; dotted arrow, deflation of the balloon.

seconds of static catheter position) was observed at the power settings used. In addition, to determine the effects of blood absorption on the detected NIRF signal in both areas of plaques and normal segments of the protease agent group, balloon occlusion, followed by saline flushing, was performed. In the protease agent group only, differences in the flush profiles were noted between plaque areas and normal segments. In plaque areas, saline flushing augmented the detected NIRF signal (Figure 4), with a peak signal increase of $74\pm18\%$. In contrast, in normal vessel segments, flushing modestly decreased the detected NIRF signal ($-38\pm6\%$ peak change; $P<0.01$ versus plaque signal changes). In control rabbits, minimal signal deviation in plaques or normal segments was detected during flushing (Figure 4).

Ex Vivo FRI of Inflammation in Atheromata

In the protease agent group, macroscopic FRI revealed NIRF signal in plaques but not in the uninjured, normal-appearing vessel segments (Figure 5). Control animals showed negligible NIRF signal from autofluorescence. The peak plaque TBR on FRI was 10.3 ± 1.8 in the protease agent group, 857% higher than the peak plaque TBR in the control group (1.8 ± 0.3; $P<0.01$). The in vivo and ex vivo peak plaque TBRs correlated well ($r=0.82$, $P<0.01$; Figure 6).

Colocalization of Microscopic NIRF Signal With Cysteine Protease and Macrophages

On fluorescence microscopy, plaque sections from the protease agent group revealed greater NIRF signal compared with sections from the control group, consistent with a low level of plaque autofluorescence at 800 nm (Figure 7). In addition, normal arterial segments from the protease group had relatively low NIRF signal, confirming that the protease-activatable agent enhanced atheromata selectively. The distinction between NIRF signal and autofluorescence was further evident on merged 2-channel fluorescence microscopy, which demonstrated green autofluorescence characteristic of elastin in all sections but only high NIRF signals in plaques from the protease agent group (Figure 7).

Further histopathological analyses revealed colocalization of the NIRF signal with cell-rich areas composed primarily of macrophages (Figure 8). Immunohistochemical detection of cathepsin B, a lysosomal cysteine protease that activates the protease agent,[4,14,15] colocalized with plaque NIRF signal and plaque macrophages (Figures 7 and 8). In contrast, minimal NIRF signal was noted in paucicellular areas of plaques. In addition, although plaques of control rabbits showed abundant macrophages and cathepsin B, minimal NIRF microscopic signal was present (data not shown).
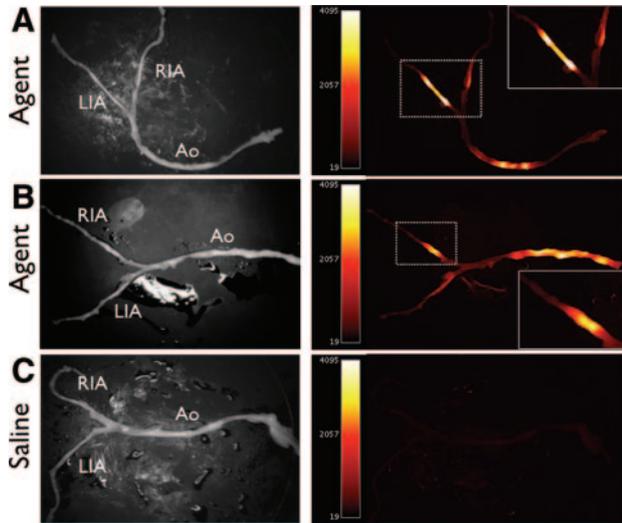
Figure 5. Ex vivo paired white light and near-infrared FRIs of atherosclerotic arteries. A and B, Augmented NIRF signal was evident in plaques in rabbits injected with the protease-activatable agent (active group). C, In contrast, control animals showed only minimal autofluorescence signal. NIRF images were windowed equally. RIA indicates right iliac artery; LIA, left iliac artery; and Ao, aorta.

Discussion

The experimental results demonstrate the detectability of inflammation-associated proteinase activity in atherosclerosis in vivo in real time using a novel intravascular NIRF catheter–sensing approach. In vivo NIRF catheter signal detection, ex vivo FRI, and microscopic NIRF signals in atherosclerotic plaques colocalized with inflammation, spe-
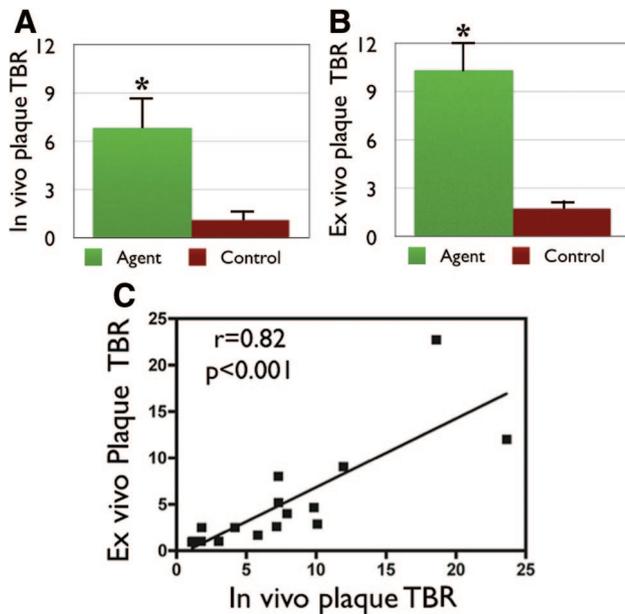

Figure 7. Correlative histopathology and fluorescence microscopy of representative arterial sections. Left, hematoxylin and eosin, ×100; middle, NIRF microscopy, ×100; right, 2-channel merged NIRF (red) and elastin autofluorescence (green), ×100. A, In plaque sections from the protease agent group, abundant NIRF signal colocalized with cell-rich areas of plaques (A) but not in the normal vessel wall (B). C, In plaque sections from the control group, negligible NIRF signal was detected, consistent with the in vivo and ex vivo NIRF imaging results. NIRF images windowed identically.

cifically augmented cysteine proteinase protein expression in macrophages.

Although assessment of protease activity in atheroma is feasible in mice via surgical exposure,[4,5] the present study used

Figure 6. Augmented NIRF signal in atheromata in the protease agent group. A, The in vivo peak plaque TBR was 558% greater in the Prosense group vs saline (6.8 ± 1.9 vs 1.3 ± 0.27, respectively; $P < 0.05$). B, The peak plaque TBR on ex vivo FRI was 856% greater in the Prosense group, with a TBR of 10.3 ± 1.8 in the agent group vs 1.8 ± 0.3 in the saline group ($P < 0.01$). C, Correlation between the in vivo and ex vivo plaque TBR was significant ($r = 0.82$, $P < 0.01$).
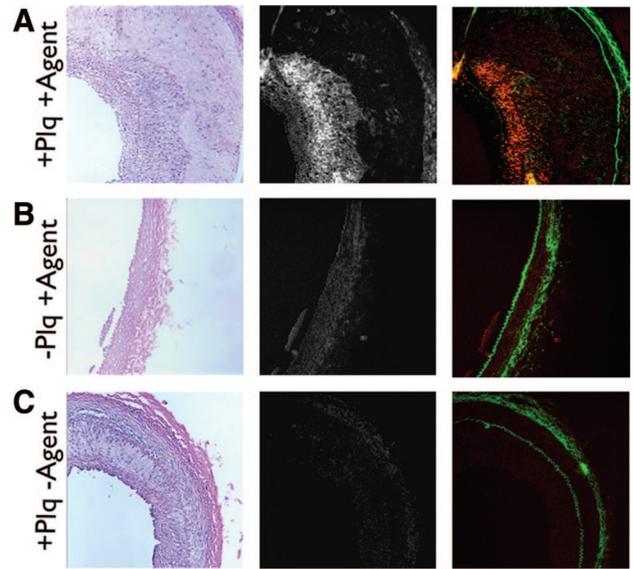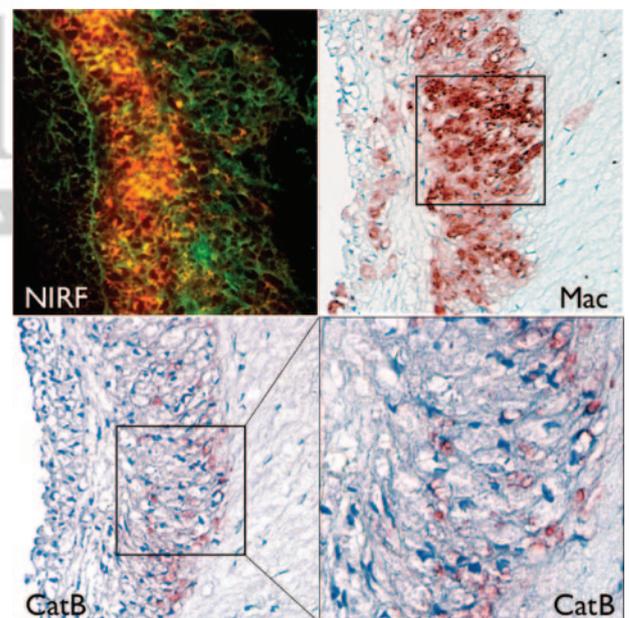

Figure 8. Augmented plaque NIRF signals colocalize with plaque macrophages and the cysteine protease cathepsin B. A, Two-channel fluorescence microscopy (×200) of plaque section in Figure 7A demonstrating abundant NIRF signal (red) overlying autofluorescence (green). Immunoreactive macrophages (Mac; ×200; A) and immunoreactive cathepsin B (CatB, ×200 and ×400; C, D) colocalize with the NIRF signal.

a novel intravascular NIRF catheter that detected plaque protease activity during catheterization of arteries of a caliber similar to human coronary arteries. Moreover, the catheter uses the same geometry and flexibility as an optical coherence tomography guidewire in use for clinical coronary arterial imaging. In addition, the current in vivo experiments demonstrated acquisition of endovascular NIRF signals through blood and during physiological blood flow as opposed to confocal microscopy approaches in which imaging is performed externally without blood interference.[16] This sensing platform visualized cysteine protease activity in real time in atherosclerotic plaques (average TBR >6) despite the presence of blood (Figure 3 and Movie I in the online-only Data Supplement). Normal arterial segments in atherosclerotic or nonatherosclerotic rabbits yielded minimal NIRF catheter–detected signal. Three synergistic factors served to augment the in vivo plaque TBR: (1) an efficient, activatable NIRF molecular imaging agent; (2) operating in the NIR window for fluorescence signal detection (efficient photon penetration up to 7 to 14 cm in transillumination mode and low tissue autofluorescence);[17] and (3) a local catheter-based system to detect fluorescent plaque signals. From an imaging agent standpoint, the highly quenched protease-activatable agent emits negligible fluorescence when initially injected. Protease-mediated cleavage of the agent produces the fluorescent signal and results in high TBRs as a result of the low background signal. In addition, 1 enzyme molecule can cleave multiple substrate copies, augmenting the efficiency of this approach. Using the catalytic properties of enzymes provides amplification not possible with the 1-to-1 stoichiometry of imaging probes based on binding of labeled inhibitors.

Studies on a phantom demonstrated that NIRF signal detection remained efficient even in the presence of blood, with a decay distance (1/e) of 500 μm compared with 700 μm in saline. In vivo studies confirmed the ability to detect efficiently NIRF signals through blood without the need for flushing or balloon occlusion. Because the average iliac artery diameter is $\approx$2 to 2.5 mm, in a 50% diameter stenosis, a centered catheter should be $\approx$600 μm away from a plaque, a distance that should readily allow NIRF signal detection (Figure 1C). Phantom measurements also demonstrated that saline displacement did not produce dramatic gains in the detected NIRF signal, as observed here in vivo (Figure 4B). Both the in vivo and phantom results suggest that the NIR window has utility for in vivo molecular imaging of atherosclerosis in vessels the size of human coronary arteries.

The NIRF signal in plaque sections was associated with both macrophages and the protease cathepsin B, a cysteine protease produced by macrophages that is a member of a proteinase family linked to atherosclerosis.[4,18–20] By promoting plaque inflammatory cell recruitment, elastinolysis and collagenolysis, apoptosis, and neoangiogenesis, cysteine proteases such as cathepsin B play a pivotal role in promoting atheroma formation, expansion, and rupture.[6–8] In the present study, cathepsin B colocalized strongly with macrophages and NIRF signal in rabbit atheromata, consistent with earlier murine atherosclerosis studies.[4,14] In addition, cysteinyl proteinases such as cathepsin B readily cleave the protease-activatable agent substrate in vitro and in vivo.[4,14,15] The current molecular imaging and histopathological results in large animals strengthen the relationship between cysteine protease activity and atherosclerosis and further validate cysteine proteases as important imaging biomarkers of plaque inflammation.

This in vivo proof-of-principle study has certain limitations. Although the imaging agent is activated predominantly by cathepsin B, other proteases may activate the agent; additional studies may clarify their relative contributions in vivo. Additional specificity for cathepsin B, if necessary, could be obtained with second-generation designs of protease-activatable agents, as recently demonstrated for cathepsin K.[16] At present, the developed catheter senses fluorescence in 90° arcs in a 1-dimensional fashion, potentially missing focal spots of high NIRF signal. To reduce sampling error, multiple NIRF catheter pullbacks were performed in each artery. In addition, only the maximum voltage was used in the in vivo data analyses to limit error during manual pullback and showed good correlation between in vivo and ex vivo data ($r=0.82$). Additional study parameters subject to further optimization include the laser power, imaging agent dose, and ideal time delay for sensing after agent injection. Advances in NIRF catheter design should enable more complete imaging (via optical fiber rotation), uniform vessel wall sampling, and automated pullbacks. The fluorescence signals detected are heavily surface weighted; further studies will determine NIRF signal variation as a function of plaque thickness. Encouragingly, the present phantom studies suggest that overlying tissue (eg, fibrous cap) will not strongly attenuate the NIRF signal. Lastly, although in vivo NIRF signal detection may be favorable in the arteries studied (2- to 2.5-mm diameter), further studies will determine NIRF signal detection capability through larger volumes of blood, as found in larger vessels or with very mildly stenotic lesions.

These studies serve to form the basis for future clinical applications of this promising technology. The imaging agent, tested safely in medium-sized animals for the first time here, appears clinically favorable from a safety profile for 2 reasons. First, the polymer backbone of the agent has already been safely investigated in clinical trials.[21] Second, the NIR fluorochromes of the agent are similar to organic fluorochromes such as indocyanine green, an agent used widely in retinal angiography and for many decades in indicator-dilution studies in humans that possesses a highly favorable safety profile.[22] In conjunction with Prosense, clinical development of NIRF catheter technology could enable coronary arterial applications such as identifying high-risk plaques harboring inflammation or assessing the biological effects of novel antiinflammatory agents on atheromata in vivo. In practice, this NIRF catheter approach could interrogate moderately stenotic coronary lesions of patients with anticipated high cardiovascular event rates such as those with established cardiovascular disease, as well as high-risk patient subsets with augmented coronary plaque inflammation such as diabetic patients.[23] Furthermore, integration of NIRF with other light-based imaging methods could yield integrated NIRF–optical coherence tomography, NIRF–optical frequency domain imaging,[24] or NIRF–NIR spectroscopy[25] catheters that enable simultaneous molecular and structural assessment of atherosclerosis in a real-time pullback fashion.

Disclosures

Drs Jaffer, Libby, and Ntziachristos have served as a consultant to VisEn Medical. Dr Weissleder is a shareholder in VisEn Medical. The other authors report no conflicts.

References

1. Hansson GK, Libby P. The immune response in atherosclerosis: a double-edged sword. *Nat Rev Immunol*. 2006;6:508–519.
2. Jaffer FA, Libby P, Weissleder R. Molecular imaging of cardiovascular disease. *Circulation*. 2007;116:1052–1061.
3. Sanz J, Fayad ZA. Imaging of atherosclerotic cardiovascular disease. *Nature*. 2008;451:953–957.
4. Chen J, Tung CH, Mahmood U, Ntziachristos V, Gyurko R, Fishman MC, Huang PL, Weissleder R. In vivo imaging of proteolytic activity in atherosclerosis. *Circulation*. 2002;105:2766–2771.
5. Deguchi JO, Aikawa M, Tung CH, Aikawa E, Kim DE, Ntziachristos V, Weissleder R, Libby P. Inflammation in atherosclerosis: visualizing matrix metalloproteinase action in macrophages in vivo. *Circulation*. 2006;114:55–62.
6. Liu J, Sukhova GK, Sun JS, Xu WH, Libby P, Shi GP. Lysosomal cysteine proteases in atherosclerosis. *Arterioscler Thromb Vasc Biol*. 2004;24:1359–1366.
7. Garcia-Touchard A, Henry TD, Sangiorgi G, Spagnoli LG, Mauriello A, Conover C, Schwartz RS. Extracellular proteases in atherosclerosis and restenosis. *Arterioscler Thromb Vasc Biol*. 2005;25:1119–1127.
8. Lutgens SP, Cleutjens KB, Daemen MJ, Heeneman S. Cathepsin cysteine proteases in cardiovascular disease. *FASEB J*. 2007;21:3029–3041.
9. Naghavi M, Libby P, Falk E, Casscells SW, Litovsky S, Rumberger J, Badimon JJ, Stefanadis C, Moreno P, Pasterkamp G, Fayad Z, Stone PH, Waxman S, Raggi P, Madjid M, Zarrabi A, Burke A, Yuan C, Fitzgerald PJ, Siscovick DS, de Korte CL, Aikawa M, Juhani Airaksinen KE, Assmann G, Becker CR, Chesebro JH, Farb A, Galis ZS, Jackson C, Jang IK, Koenig W, Lodder RA, March K, Demirovic J, Navab M, Priori SG, Rekhter MD, Bahr R, Grundy SM, Mehran R, Colombo A, Boerwinkle E, Ballantyne C, Insull W Jr, Schwartz RS, Vogel R, Serruys PW, Hansson GK, Faxon DP, Kaul S, Drexler H, Greenland P, Muller JE, Virmani R, Ridker PM, Zipes DP, Shah PK, Willerson JT. From vulnerable plaque to vulnerable patient: a call for new definitions and risk assessment strategies: part I. *Circulation*. 2003;108:1664–1672.
10. Zhu B, Jaffer FA, Ntziachristos V, Weissleder R. Development of a near infrared fluorescence catheter: operating characteristics and feasibility for atherosclerotic plaque detection. *J Phys D Appl Phys*. 2005;38:2701–2707.
11. Fujimoto JG, Pitris C, Boppart SA, Brezinski ME. Optical coherence tomography: an emerging technology for biomedical imaging and optical biopsy. *Neoplasia*. 2000;2:9–25.
12. Baeten J, Niedre M, Dunham J, Ntziachristos V. Development of fluorescent materials for diffuse fluorescence tomography standards and phantoms. *Opt Express*. 2007;15:8681–8694.
13. Cheong W, Prahl S, Welch A. A review of the optical-properties of biological tissues. *IEEE J Quantum Electron*. 1990;26:2166–2185.
14. Aikawa E, Nahrendorf M, Sosnovik D, Lok VM, Jaffer FA, Aikawa M, Weissleder R. Multimodality molecular imaging identifies proteolytic and osteogenic activities in early aortic valve disease. *Circulation*. 2007;115:377–386.
15. Weissleder R, Tung CH, Mahmood U, Bogdanov A Jr. In vivo imaging of tumors with protease-activated near-infrared fluorescent probes. *Nat Biotechnol*. 1999;17:375–378.
16. Jaffer FA, Kim DE, Quinti L, Tung CH, Aikawa E, Pande AN, Kohler RH, Shi GP, Libby P, Weissleder R. Optical visualization of cathepsin K activity in atherosclerosis with a novel, protease-activatable fluorescence sensor. *Circulation*. 2007;115:2292–2298.
17. Weissleder R, Ntziachristos V. Shedding light onto live molecular targets. *Nat Med*. 2003;9:123–128.
18. Reddy VY, Zhang QY, Weiss SJ. Pericellular mobilization of the tissue-destructive cysteine proteinases, cathepsins B, L, and S, by human monocyte-derived macrophages. *Proc Natl Acad Sci U S A*. 1995;92:3849–3853.
19. Li W, Dalen H, Eaton JW, Yuan XM. Apoptotic death of inflammatory cells in human atheroma. *Arterioscler Thromb Vasc Biol*. 2001;21:1124–1130.
20. Papaspyridonos M, Smith A, Burnand KG, Taylor P, Padayachee S, Suckling KE, James CH, Greaves DR, Patel L. Novel candidate genes in unstable areas of human atherosclerotic plaques. *Arterioscler Thromb Vasc Biol*. 2006;26:1837–1844.
21. Callahan RJ, Bogdanov A Jr, Fischman AJ, Brady TJ, Weissleder R. Preclinical evaluation and phase I clinical trial of a ^{99m}Tc-labeled synthetic polymer used in blood pool imaging. *AJR Am J Roentgenol*. 1998;171:137–143.
22. Hope-Ross M, Yannuzzi LA, Gragoudas ES, Guyer DR, Slakter JS, Sorenson JA, Krupsky S, Orlock DA, Puliafito CA. Adverse reactions due to indocyanine green. *Ophthalmology*. 1994;101:529–533.
23. Moreno PR, Murcia AM, Palacios IF, Leon MN, Bernardi VH, Fuster V, Fallon JT. Coronary composition and macrophage infiltration in atherectomy specimens from patients with diabetes mellitus. *Circulation*. 2000;102:2180–2184.
24. Yun SH, Tearney GJ, Vakoc BJ, Shishkov M, Oh WY, Desjardins AE, Suter MJ, Chan RC, Evans JA, Jang IK, Nishioka NS, de Boer JF, Bouma BE. Comprehensive volumetric optical microscopy in vivo. *Nat Med*. 2006;12:1429–1433.
25. Moreno PR, Lodder RA, Purushothaman KR, Charash WE, O'Connor WN, Muller JE. Detection of lipid pool, thin fibrous cap, and inflammatory cells in human aortic atherosclerotic plaques by near-infrared spectroscopy. *Circulation*. 2002;105:923–927.

CLINICAL PERSPECTIVE

Inflammation critically modulates atherosclerosis and is implicated in plaque rupture, a leading cause of myocardial infarction. Clinical methods to sense plaque inflammation in vivo, however, remain limited, particularly in small coronary arteries. Here, we present a new catheter-based intravascular near-infrared fluorescence (NIRF) sensing method to sense inflammation in experimental atherosclerosis in human coronary–sized vessels. In conjunction with an injectable cysteine protease–activatable NIRF agent, the fluorescence catheter sensitively and atraumatically detected NIRF signals in plaques during real-time pullback and through blood. In vivo NIRF signals were detected without the need for balloon occlusion or saline flushing and correlated well with ex vivo NIRF data. On histological analyses, microscopic NIRF signals colocalized with inflammatory plaque macrophages and plaque cathepsin B, a cysteine protease implicated in atherosclerosis. The intravascular NIRF catheter and protease-activatable agent strategy could allow detection of inflamed plaques and high-risk patients and could provide a biological readout for antiinflammatory atherosclerosis therapies.